

Spectroscopy and IVR in the S₁ State of Jet-Cooled *p*-Alkoxyphenols

G. N. Patwari, S. Doraiswamy, and S. Wategaonkar*

Department of Chemical Sciences, Tata Institute of Fundamental Research, Homi Bhabha Road, Colaba, Mumbai 400005, India

Received: March 3, 2000; In Final Form: June 5, 2000

Vibronic spectroscopy and intramolecular vibrational relaxation studies were carried out on jet-cooled hydroquinone, *p*-methoxyphenol, and *p*-ethoxyphenol using laser-induced fluorescence measurements. The *cis* and *trans* isomeric forms of all three compounds exist even under jet-cooled conditions. Hole-burning spectroscopy was used to separate the transitions due to each of them. Vibrational assignments were made with the help of dispersed fluorescence spectra after single vibronic excitations. The fluorescence spectra were also used to deduce the onset of mode mixing, a precursor to IVR. The IVR onset in the case of hydroquinone was quite high, i.e., 1650 cm⁻¹, and it decreased substantially in *p*-methoxyphenol. It did not decrease any further for *p*-ethoxyphenol. One of the objectives of this study was to compare the IVR behavior in this series to that in *p*-alkoxyanilines, or more specifically, to compare the effect of the presence of an -OH group vs an -NH₂ group in the para position on IVR.

1. Introduction

Developing an understanding of the dynamics of intramolecular processes in isolated gaseous molecules is one of the important issues in the field of chemical physics. Intramolecular vibrational redistribution (IVR) plays a pivotal role in this regard. Recent advances in experiment and theory have achieved some success in the understanding and control of IVR dynamics in relatively small systems.^{1–5} However, dynamics of IVR are substantially elusive in polyatomics. The ultimate goal in this regard has been understanding the IVR dynamics and formulating propensity rules to control it at chemically significant energies. IVR studies on various alkyl-chain-substituted benzenes (termed “ring-tail” compounds), viz., alkylbenzenes,^{6–8} *p*-alkylanilines,⁹ phenoxyalkanes,¹⁰ phenylalkynes,¹¹ and *p*-alkylphenols,¹² have led to the conclusion that the energy flow is from the ring (benzene ring) to the tail (alkyl chain). The increase in the rate of IVR with alkyl-chain length was attributed to an increase in the density of states with alkyl chain. Theoretical studies by Gruner and Brumer¹³ on alkylbenzenes have shown that the ring-based vibrational modes and the torsional vibrations of the alkyl chain are strongly coupled.

Various groups have investigated IVR in various substituted benzenes with the aim of understanding the effect of substituents and symmetry on IVR.^{14–24} These studies only ascertained the fact that the density of states influences IVR. The onset of IVR in most cases was found to be around 800 cm⁻¹ or less, with the exceptions of *p*-difluorobenzene,^{14–16} *p*-aminophenol,²⁵ and *p*-dimethoxybenzene.²⁶ In all of the substituted benzenes that have been investigated so far, the alkyl chain was attached to the benzene ring with a single bond with very little barrier for rotation. These systems presumably have strong Coriolis coupling between the ring and the rotor levels, which leads to fast IVR. In the case of *p*-methylaniline, the coupling between the -NH₂ inversion and the -CH₃ rotor levels in the excited state was probed spectroscopically, and the results suggested

that this coupling could affect the rates of IVR in these molecules.²⁷ IVR studies on compounds with weak coupling between the ring-based vibrational modes and the torsions of the alkyl chain are very sparse.

In para-substituted benzenes with substituents carrying a lone pair of electrons (X̄), the out-of-plane “p” orbital has antibonding and nonbonding contributions to the HOMO and the LUMO, respectively. Electronic excitation thus leads to a stiffening of the C-X̄ bond, giving more quinoidal character to the molecule. This raises the C-X̄ torsional barrier and reduces the coupling between the ring modes and the vibrational modes of the alkyl chain. The onset of IVR in such systems is expected to be at relatively higher energies than that in other systems. Earlier, we reported IVR studies on *p*-alkoxyanilines.^{25,28,29} The results for *p*-aminophenol were encouraging in this regard, and the onset of IVR was observed at much higher energies than in the case of molecules with comparable density of states but lesser quinoidal character.²⁵ When the phenolic hydrogen was replaced with an alkyl group to increase the density of states, the result was a dramatic reduction in the quinoidal character, and the observed onset of IVR became nearly comparable with that of the other alkyl-substituted benzene derivatives.^{28,29} This suggests that the phenolic group could be the major contributor to the quinoidal character. In view of this, IVR investigations on a new series of compounds, viz., *p*-alkoxyphenols, were undertaken. The objective was to keep the phenolic group on the benzene ring intact and to vary the density of states by increasing the alkyl-chain length of the -OR group in the para position.

In this paper, we report spectroscopic and IVR studies on hydroquinone, *p*-methoxyphenol, and *p*-ethoxyphenol, the first three members of the *p*-alkoxyphenol series. Each of these compounds exists in *trans* and *cis* isomeric forms. The spectroscopy of *trans*- and *cis*-hydroquinone has already been reported,^{30–33} but there has not been any report on the spectroscopy of *p*-methoxyphenol and *p*-ethoxyphenol. Hence, vibronic spectroscopy was performed to characterize their vibrational levels in the excited state. Spectral features of the dispersed fluorescence spectra were used to infer IVR.

* Author to whom correspondence should be addressed. E-mail: sanwat@tifr.res.in. Fax: +91-22-2152110.

There have been numerous reports in the literature on isomer-dependent IVR.^{9,26,29,34} In almost all of the cases in which isomer-dependent IVR has been reported, the isomers are the consequence of the various conformations of the alkyl chain attached to the benzene ring. In these systems, the changes in the potential along various ring-based vibrational modes are very small, and the effect is mainly due to the long-range interactions of the alkyl chain with benzene ring. In the present series, each compound exists as *trans* and *cis* isomers, which may have different potentials for various ring-based modes. Because the density of states is expected to be almost identical for both the isomers, it would be possible to study the effect of the electronic structure (potential) on IVR. The differences in the electronic structures or lack of it can be probed using vibronic spectroscopy. Subsequently, any observed differences in the IVR behavior could be attributed to the differences in the electronic structures of the respective isomer, as observed in the case of *p*-dimethoxybenzene.²⁶

2. Experimental Section

The details of the experimental setup have been reported elsewhere.^{25,35} Briefly, the experiments were carried out using a 100- μm -diameter pulsed nozzle driven by a pulsed valve driver (General Valve Corporation; IOTA ONE; 70- Ω solenoid coil) and 10 atm stagnation pressure of He buffer gas. The chamber pressure during the experiments was about 2×10^{-5} Torr. The reagents were heated to generate enough vapor pressure in the jet to record spectra with a good signal-to-noise ratio. A Nd³⁺:YAG (Quantel YG 781C) pumped dye laser (Molelectron DL-18P; R590+R610 dye; wavelength region = 2760–2980 Å) was the excitation source for the excitation spectra and the dispersed fluorescence spectra. The line width of the dye laser was $\sim 0.3 \text{ cm}^{-1}$, and the typical pulse energies used were $\leq 50 \mu\text{J}$. The total fluorescence was detected by a PMT/filter combination (1P28; WG-320/305) for recording the excitation spectra. The dispersed fluorescence was monitored using a monochromator (ARC-VM505; 0.5 m) and PMT (Hamamatsu R-943). The typical resolution in the dispersed fluorescence spectra was 10–15 cm^{-1} . Signal was digitized and averaged using a digital storage oscilloscope (Lecroy 9450A). Vibronic spectroscopy of the individual isomers was accomplished using hole-burning spectroscopy. The total fluorescence from the band origin excitation of one of the isomers was probed using a delayed probe pulse (Quantel TDL-70; $\sim 20 \mu\text{J}$), and a pump laser (Molelectron DL-18P; $\sim 500 \mu\text{J}$) scanned the entire wavelength range of the excitation spectrum. Hydroquinone, *p*-methoxyphenol, and *p*-ethoxyphenol were obtained from S. D. Fine Chemicals and were used as obtained. Helium was taken from commercial tanks without further purification.

3. Results

Fluorescence Excitation Spectra. Fluorescence excitation spectra and vibronic assignments of *trans* and *cis* isomers of hydroquinone have been reported earlier.³⁵ For the sake of comparison, the excitation spectrum is shown in Figure 1a, and Table 1 lists all of the observed transitions and their assignments in the S₁ state. It can be seen from Table 1 that the energies of various vibrational modes for both of the isomers are within a few wavenumbers of each other. The excitation spectrum comprises transitions involving primarily three totally symmetric modes, viz., 6a, 1, and 7a. A progression in mode 6a up to $\nu' = 3$ was observed on the band origin as well as on the 1¹ and 7a¹ transitions.

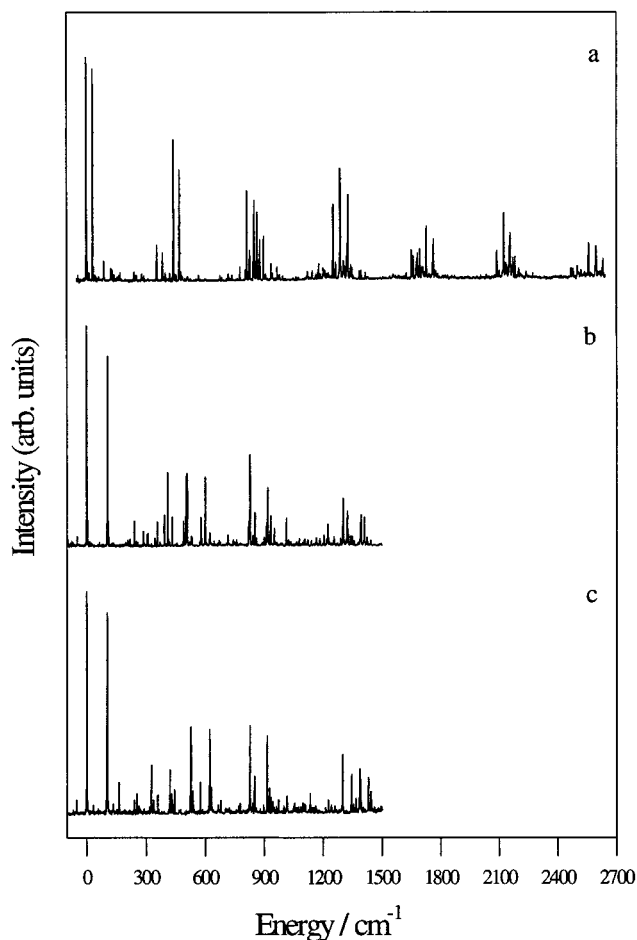


Figure 1. Fluorescence excitation of (a) hydroquinone, (b) *p*-methoxyphenol, and (c) *p*-ethoxyphenol plotted with respect to the band origins of their *trans* isomer at 33 508, 33 573, and 33 557 cm^{-1} , respectively. The spectra were normalized with respect to laser power.

Traces b and c of Figure 1 depict the fluorescence excitation spectra of *p*-methoxyphenol and *p*-ethoxyphenol, respectively. The two intense peaks on the red side in each spectrum were assigned as the band origins of the two isomers. Of the two band origin transitions, the lower-energy transition was assigned to the *trans* isomer by analogy with hydroquinone^{33,35} and *p*-dimethoxybenzene.²⁶ The separations between the *trans* and *cis* band origins were 106 and 103 cm^{-1} in *p*-methoxyphenol and *p*-ethoxyphenol, respectively. Hole-burning spectroscopy was carried out to separate the transitions belonging to individual isomers in each of the excitation spectra. Tables 2 and 3 list relative intensities and assignments of observed transitions in the excitation spectra of *p*-methoxyphenol and *p*-ethoxyphenol, respectively. The assignments were carried out with the help of the dispersed fluorescence spectra. In both cases, the relative intensities and frequencies of various observed vibrational modes were similar for the two isomers, as in the case of hydroquinone.

It is apparent from Figure 1 that spectral characteristics change from hydroquinone to *p*-ethoxyphenol. The number of allowed transitions increases as a result of the reduction in symmetry due to substitution of bulky alkyl groups off the C₂ axis. The Franck–Condon activity also changes from hydroquinone to *p*-ethoxyphenol. The length of the progression in mode 6a is reduced down the series of molecules, and the intensity of the band origins is significantly higher relative to that of the rest of the transitions in the cases of *p*-methoxyphenol and *p*-ethoxyphenol.

TABLE 1: Observed Vibrational Transitions and Their Assignments in the S_1 State of Hydroquinone^a

$\Delta\nu$ (cm ⁻¹) trans ^b	rel. int.	$\Delta\nu$ (cm ⁻¹) cis ^c	rel. int.	assignment
0	100	0	100	0 ₀ ^o
357	15	353	13	16a ₀ ²
441	62	440	49	6a ₀ ¹
788	6	781	5	—
822	40	828	37	1 ₀ ¹
836	16	834	6	9b ₀ ²
857	20	858	17	16b ₀ ²
876	30	877	21	6a ₀ ²
946	7	944	5	—
1250	35	1254 ^d	56	6a ₀ ¹ 1 ₀ ¹
1263		1272		—
1286 ^d	53	1295	42	7a ₀ ¹
1322			18	6a ₀ ³
1639	14	1653	15	1 ₀ ²
1649	11			9b ₀ ² 1 ₀ ¹
1670	12			9b ₀ ⁴
1683	14			1 ₀ ¹ 16b ₀ ²
1717	25	1719	20	6a ₀ ¹ 7a ₀ ¹
2071	14			—
2107	32	2107	23	1 ₀ ¹ 7a ₀ ¹
2153	10			6a ₀ ² 7a ₀ ¹
2554	17	2565	17	6a ₀ ¹ 1 ₀ ¹ 7a ₀ ¹

^a The relative intensities of the trans and the cis band origin transitions were 1 and 0.95, respectively. ^b $\Delta\nu$ with respect to the band origin at 33 508 cm⁻¹. ^c $\Delta\nu$ with respect to the band origin at 33 540 cm⁻¹. ^d Overlapping transitions.

Dispersed Fluorescence Spectra. The dispersed fluorescence (DF) spectra were recorded for most of the transitions observed in the excitation spectra for all three molecules. These spectra provide information about the extent of vibrational-state mixing in the excited state and aid the vibrational assignments in the S_1 and S_0 states. For a given vibrational mode, the $\Delta\nu = 0$ transition in the DF spectrum is usually the strongest transition, and it also acts as a pseudo-origin for the rest of the spectrum when the potentials in the S_0 and S_1 states are similar. In addition, when the potentials are relatively shifted, because of a change in the equilibrium geometry, a progression is observed.

Figure 2 shows the DF spectra following band-origin excitation of the trans and the cis isomers of all three molecules. The DF spectra of the isomers are remarkably similar in each case, with no apparent change in the frequencies or the Franck–Condon activity in various observed vibrational modes. Furthermore, just as in the case of the excitation spectra, the characteristics of the DF spectra also change down the series. Table 4 summarizes the vibronic assignments for both of the isomers of all three molecules.

Figure 3 shows the DF spectra of various vibronic excitations of *trans*-hydroquinone. Traces a and b of Figure 3 depict the DF spectra of the 6a₀¹ and 6a₀² excitations, respectively. The salient features were a long progression up to $\nu'' = 6$ in mode 6a that had a bimodal Franck–Condon intensity distribution with a minimum at $\Delta\nu = 0$. The DF spectrum of the 7a₀¹ (1286 cm⁻¹) excitation is presented in Figure 3c. This spectrum is very similar to the band-origin DF spectrum (Figure 3a), except that the 7a₀¹ transition is stronger and acts as a pseudo-origin. Figure 3d is the DF spectrum of the 1₀² (1639 cm⁻¹) excitation. The most intense peak at 853 cm⁻¹ is the 1₀² transition. Although most of the discrete transitions in the spectrum can

TABLE 2: Observed Vibrational Transitions and Their Assignments in the S_1 State of *p*-Methoxyphenol^a

$\Delta\nu$ (cm ⁻¹) trans ^b	rel. int.	$\Delta\nu$ (cm ⁻¹) cis ^c	rel. int.	assignment
0	100	0	100	0 ₀ ^o
241	12			15 ₀ ¹
285	7			
310	6			
357	11	327	16	16a ₀ ²
393	15	385	14	9b ₀ ¹
410	34	407	39	6a ₀ ¹
		477	5	11 ₀ ²
506	33	495	37	10b ₀ ²
579	13			6b ₀ ¹
718	5			16a ₀ ⁴
761	4			16a ₀ ² 6a ₀ ¹
		806	11	
822	12			6a ₀ ²
		813 ^d	31	6a ₀ ² & 1 ₀ ¹
829	42			1 ₀ ¹
		829	16	10a ₀ ¹ X ₀ ¹
853	16	847 ^e	16	10a ₀ ²
		908	15	6a ₀ ¹ 10b ₀ ²
1221	10	1194	18	9b ₀ ¹ 1 ₀ ¹
		1217	9	6a ₀ ¹ 1 ₀ ¹
		1285	14	6a ₀ ¹ 9b ₀ ¹ 10b ₀ ²
1298	22	1299	16	7a ₀ ¹
1319	16			14 ₀ ¹
1345	5	1313	5	10b ₀ ² 1 ₀ ¹
1628	16			
1653	12	1619	9	1 ₀ ²
1692	7	1638	10	1 ₀ ¹ 16a ₂ ⁰ 10b ₂ ⁰
		1655	6	1 ₀ ¹ 16b ₂ ⁰

^a The relative intensities of the trans and the cis band origin transitions were 1 and 0.86, respectively. ^b $\Delta\nu$ with respect to the band origin at 33 573 cm⁻¹. ^c $\Delta\nu$ with respect to the band origin at 33 679 cm⁻¹. ^d Overlapping transitions. ^e In addition, it is mixed with some other state.

be assigned to the initially excited state, a considerable amount of spectral congestion to the red side of the band origin is also evident. The next two traces, viz., 3e and 3f, show the DF spectra of the 1717 cm⁻¹ (6a₀¹ 7a₀¹) and the 2107 cm⁻¹ (1₀¹ 7a₀¹) excitations. The spectral congestion increases progressively with energy, and for the latter excitation, the spectrum is completely devoid of any discrete transitions, with very little intensity in the resonance transition. The 1717 cm⁻¹ excitation is a combination band of 6a₀¹ 7a₀¹, and the observed intensity distribution pattern of various discrete bands reflects just that. The DF spectra of corresponding excitations of *cis*-hydroquinone are almost identical to those of their trans counterparts in all respects, including the onset and extent of IVR.

Figure 4 shows the DF spectra of various vibronic excitations of *trans*-methoxyphenol. Figure 4a shows the DF spectrum of the 241 cm⁻¹ (15₀¹) excitation. The intense transition at 243 cm⁻¹ that acts as a pseudo-origin gives the corresponding ground-state frequency. The DF spectrum of the 357 cm⁻¹ (16a₀²) excitation (Figure 4b) shows the most intense transition at 825 cm⁻¹, corresponding to the 16a₂² transition. In addition to this, two strong transitions are observed at 560 and 662 cm⁻¹ on which the entire band origin DF spectrum can be mapped. The 662 cm⁻¹ transition is assigned as the 4₁⁰ transition. This out-of-plane bending mode has a mode description comparable

TABLE 3: Observed Vibrational Transitions and Their Assignments in the S_1 State of *p*-Ethoxyphenol

$\Delta\nu$ (cm ⁻¹) trans ^b	rel. int.	$\Delta\nu$ (cm ⁻¹) cis ^c	rel. int.	assignment
0	100	0	100	0 ₀ ⁰
163	15	149	11	15 ₀ ¹
326	22	316	22	6a ₀ ¹
359	9	340	13	16a ₀ ²
431	10	420	9	
527	39	519	42	10b ₀ ²
575	15	563	5	6b ₀ ²
678	7	674	6	
828	40	814	39	1 ₀ ¹
		826	13	10a ₀ ¹ X ₀ ¹
		835	7	6a ₀ ¹ 10b ₀ ²
851	17			10a ₀ ²
		916	9	18a ₀ ¹
976	7			15 ₀ ¹ 1 ₀ ¹
1137	10	1126	8	6a ₀ ¹ 1 ₀ ¹
1302	27	1285	23	7a ₀ ¹
		1290	18	14 ₀ ¹
1347	18	1328	19	1 ₀ ¹ 10b ₀ ²
1445	11			

^a The relative intensities of the trans and the cis band origin transitions were 1 and 0.91, respectively. ^b $\Delta\nu$ with respect to the band origin at 33 557 cm⁻¹. ^c $\Delta\nu$ with respect to the band origin at 33 660 cm⁻¹.

to that of 16a, and the appearance of this transition suggests that these two modes are strongly mixed in the excited state. The 560 cm⁻¹ transition can not be assigned categorically to any mode, but it could be a $\Delta\nu = 2$ transition in the $-\text{OCH}_3$ torsional mode.³⁶ Figure 4c shows the DF spectrum of the 393 cm⁻¹ excitation corresponding to the 9b₀¹ transition. In addition to the 9b₀¹ transition at 373 cm⁻¹, a fairly strong peak is also observed at 485 cm⁻¹, corresponding to the 15₀² frequency, suggesting that these two C–X in-plane bending modes are strongly mixed in the excited state. The DF spectrum of the 6 a₀¹ (410 cm⁻¹) excitation is presented in Figure 4d. The 6a₀¹ transition appears at 433 cm⁻¹, along with a weak progression up to $\nu'' = 3$, which is considerably shorter than that observed in the case of hydroquinone. The appearance of the spectrum is somewhat deceptive because of the overlapping of the 6a₂¹ with the 1₁⁰ and the 6a₃¹ with the 6a₁¹ transitions. The shortening of the progression in mode 6a upon substitution of the phenolic hydrogen with a methyl group is similar to that observed in the cases of *p*-aminophenol and *p*-methoxyaniline.^{25,28}

Traces e and f of Figure 4 are the DF spectra of the 10b₀² (506 cm⁻¹) and 6b₀¹ (579 cm⁻¹) excitations, respectively. The corresponding $\Delta\nu = 0$ transitions are observed at 527 and 644 cm⁻¹. A short progression is also observed in 10b mode in the 10b₀² spectrum. The DF spectrum of the 1₀¹ (829 cm⁻¹) excitation is presented in Figure 4g. A progression up to $\nu'' = 2$ is observed in the excited mode, with a minimum at $\Delta\nu = 0$ transition. Very weak spectral congestion is also observed in this spectrum to the red of the $\Delta\nu = 0$ transition. The DF spectrum following the 853 cm⁻¹ (10a₀²) excitation is shown in Figure 4h. The spectrum shows two prominent transitions at 495 and 1590 cm⁻¹ upon which the band origin DF spectrum can be mapped. On the basis of the characteristics of the 10a mode,^{36,37} the 1590 cm⁻¹ transition is assigned as 10a₂². The 495 cm⁻¹ transition is most likely to be 16b₁¹, which appears as

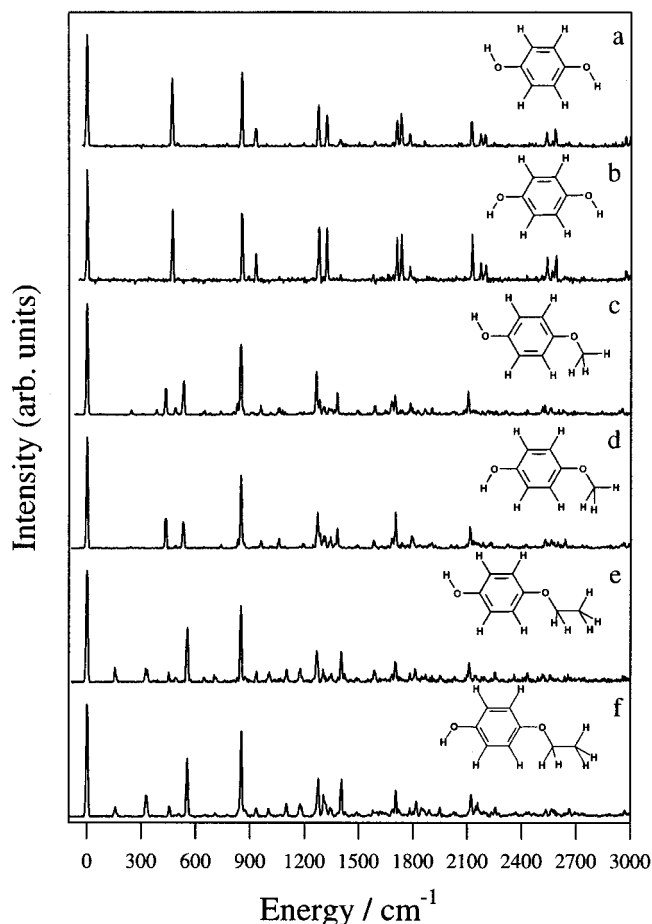


Figure 2. Band origin dispersed fluorescence spectra of (a) *trans*-hydroquinone, (b) *cis*-hydroquinone, (c) *trans*-*p*-methoxyphenol, (d) *cis*-*p*-methoxyphenol, (e) *trans*-*p*-ethoxyphenol, and (f) *cis*-*p*-ethoxyphenol. The band-pass of the monochromator was 10 cm⁻¹ for all of the spectra. For better presentation, the excitation transitions are aligned, and the spectra are plotted on a relative energy scale.

a result of mode mixing in the excited state. The spectrum also shows an enhanced spectral congestion, indicating that IVR is operative at this energy although it is restrictive. The DF spectrum of the 1221 cm⁻¹ (9b₀¹ 1₀¹) excitation (Figure 4i) is a bare continuum devoid of any discrete transitions and with very little fluorescence at the resonance position, suggesting that the IVR is dissipative at this energy.

Figure 5 shows the DF spectra of various vibronic excitations of *cis*-methoxyphenol. In the DF spectrum of the 327 cm⁻¹ (16 a₀²) excitation (Figure 5a), in addition to the 16a₂² transition at 832 cm⁻¹, strong transitions are also observed at 398 and 669 cm⁻¹. The 669 cm⁻¹ transition is assigned as 4₁⁰ by analogy with the *trans* isomer. In both isomers, the 16a₂² level in the excited state is strongly mixed with mode 4, along with a few other modes (such as the 398 cm⁻¹ transition in this case and the 560 cm⁻¹ in the *trans* isomer), but the extent of mixing is different. Similarly, in the case of the 9b₀¹ (385 cm⁻¹) excitation (Figure 5b), in addition to the intense $\Delta\nu = 0$ transition at 375 cm⁻¹, transitions at 480 and 669 cm⁻¹ are fairly strong. The Franck–Condon activity in this spectrum is also quite different compared to that in the corresponding excitation of the *trans* isomer. These observations indicate that there are certain definite differences in mode mixing in the *cis* and *trans* isomers of *p*-methoxyphenol. The DF spectra of the 6a₀¹ (407 cm⁻¹) and 10b₀² (495 cm⁻¹) excitations (Figure 5c and 5d, respectively) are very similar to those of their *trans* counterparts.

TABLE 4: Vibrational Assignments of the Excited- and Ground-State Fundamentals of the Trans and Cis Isomers of Hydroquinone, *p*-Methoxyphenol, and *p*-Ethoxyphenol

mode	hydroquinone				<i>p</i> -methoxyphenol				<i>p</i> -ethoxyphenol			
	trans		cis		trans		cis		trans		cis	
	ν'	ν''	ν'	ν''	ν'	ν''	ν'	ν''	ν'	ν''	ν'	ν''
15					241	243			163	152	149	157
16a ($\nu = 2$)	357		353		357	825	327	832	359	828	340	832
9b	836/2		834/2		393	373	385	375	333		335	
6a	441	469	440	469	410	433	407	433	326	323	316	326
11 ($\nu = 2$)							477		450		453	
10b ($\nu = 2$)					506	527	495	531	527	553	519	555
6b					579	644		644	575	643	563	
4						662		669				
1	822	853	828	852	829	848	813	848	828	848	814	854
10a ($\nu = 2$)					853	1590	847	780	851	1595		
16b ($\nu = 2$)	857	1089	834	858	1070							
7a	1286	1272	1295	1274	1298	1261	1299	1269	1302	1266	1285	1275

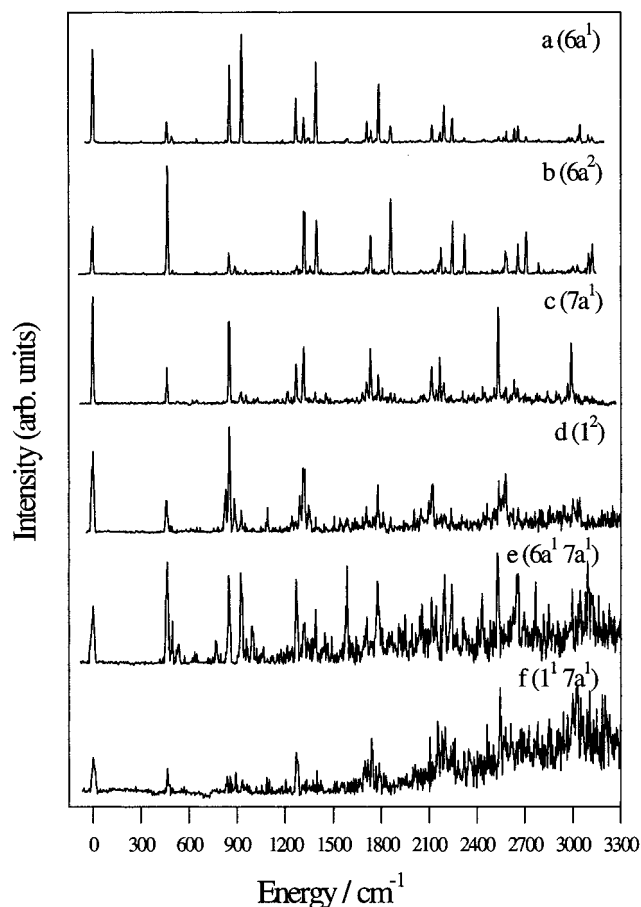
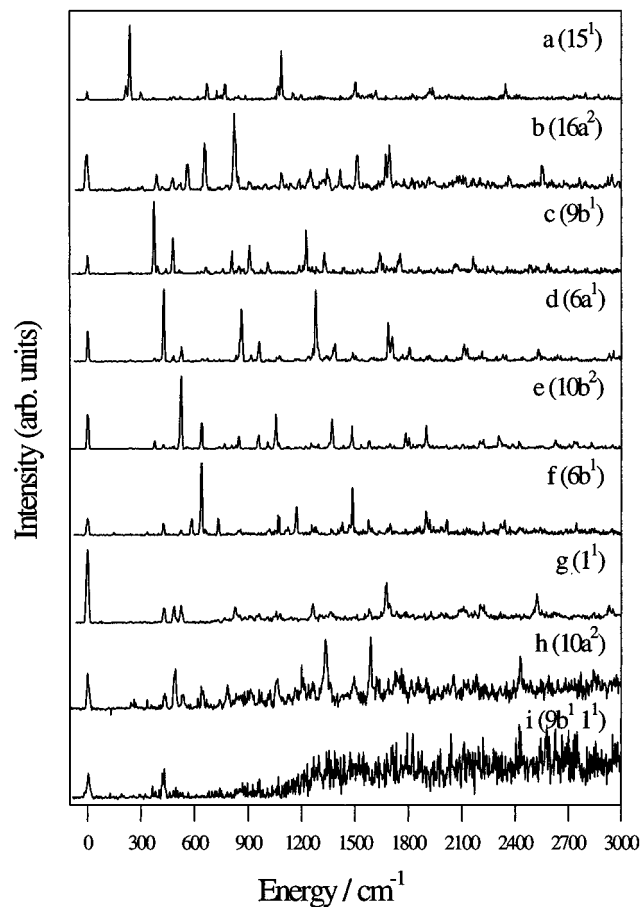
**Figure 3.** Dispersed fluorescence spectra following excitation of the (a) 441, (b) 876, (c) 1268, (d) 1639, (e) 1717, and (f) 2107 cm^{-1} transitions of *trans*-hydroquinone. The band-pass of monochromator was 10 cm^{-1} for a–d and 15 cm^{-1} for e and f. For better presentation, the excitation transitions are aligned, and the spectra are plotted on a relative energy scale.

Figure 5e is the DF spectrum of the 813 cm^{-1} excitation, which is an overlapping transition of the 1_0^1 and $6a_0^2$ transitions. Some amount of spectral congestion in the form of a continuum is also observed to the red side of the band origin. Trace f of Figure 5 represents the DF spectrum of the 829 cm^{-1} excitation. The spectrum consisted of two strong transitions at 780 and 860 cm^{-1} , on which the band origin DF spectrum repeated. Because 780 cm^{-1} corresponds to the 10a mode in the ground state, on the basis of symmetry considerations, the transition must be 10

**Figure 4.** Dispersed fluorescence spectra following excitation of the (a) 241, (b) 357, (c) 393, (d) 410, (e) 506, (f) 579, (g) 829, (h) 853, and (i) 1221 cm^{-1} transitions of *trans*-*p*-methoxyphenol. The band-pass of monochromator was 10 cm^{-1} for a–e and 15 cm^{-1} for f–i. For better presentation, the excitation transitions are aligned, and the spectra are plotted on a relative energy scale.

a_1^1 . This dictates that the 829 cm^{-1} excitation must be a combination of $10a_0^1$ with a single quantum excitation in some other non-totally symmetric mode, X, i.e., $10a_0^1 X_0^1$. The 860 cm^{-1} transition must then be the X_1^1 transition. A similar situation was also encountered in the 847 cm^{-1} excitation (Figure 5g). This spectrum shows features of both $10a_0^2$ as well as $10a_0^1 X_0^1$ excitations, i.e., the 780 cm^{-1} transition ($10a_0^1$) as well as the 1560 cm^{-1} transition ($10a_0^2$) are equally strong. A definite assignment of the 829 and the 847 cm^{-1} excitations is

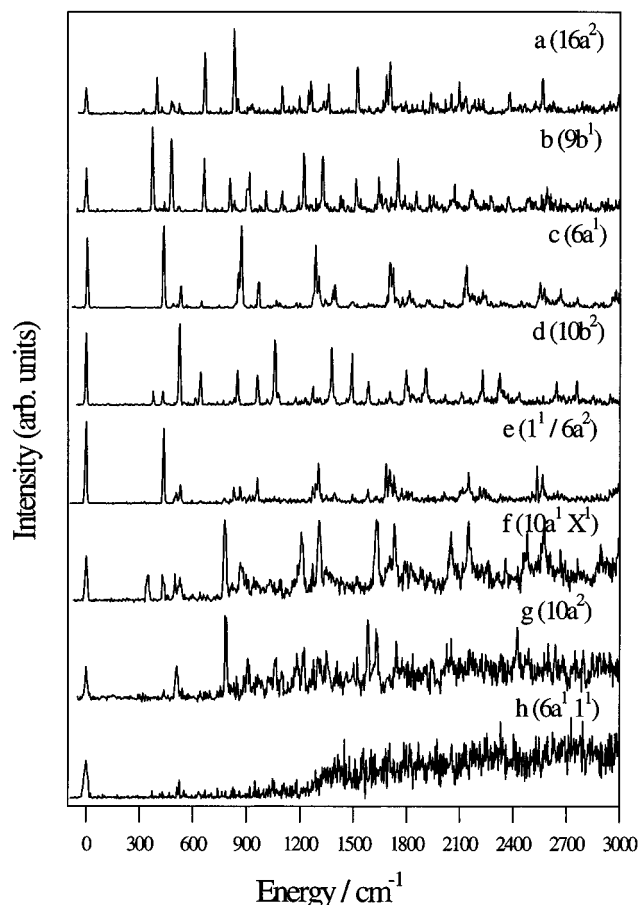


Figure 5. Dispersed fluorescence spectra following excitation of the (a) 327, (b) 385, (c) 407, (d) 495, (e) 813, (f) 829, (g) 847, and (h) 1217 cm^{-1} transitions of *cis-p*-methoxyphenol. The band-pass of monochromator was 10 cm^{-1} for a–e and 15 cm^{-1} for f–h. For better presentation, the excitation transitions are aligned, and the spectra are plotted on a relative energy scale.

difficult, but it is obvious that mode mixing is significant in this energy range. Very few discrete transitions are seen, and both of the spectra suffer from severe spectral congestion. The DF spectrum of the 1221 cm^{-1} ($6a_0^1 1_0^1$) excitation (Figure 5h) is a bare continuum similar to that of its trans counterpart.

Figure 6 shows the DF spectra of various vibronic excitations of *trans*-ethoxyphenol. Most of the spectroscopic assignments are quite straightforward and do not require any discussion. Figure 6b shows the DF spectrum of the 326 cm^{-1} excitation. The intense $\Delta v = 0$ transition at 323 cm^{-1} that acts as a pseudo-origin is assigned to mode $6a$ by analogy with *p*-ethoxyaniline.²⁸ In the DF spectrum of the $10b_0^2$ (527 cm^{-1}) excitation (Figure 6d), in addition to the $10b_2^2$ and $10b_4^2$ transitions at 553 and 1105 cm^{-1} , respectively, a strong transition is observed at 518 cm^{-1} . It is assigned to the $16b_1^1$ transition, the appearance of which could be ascribed to its mixing with the $10b^2$ level in the excited state. The DF spectra of the 828 (1_0^1) and 851 cm^{-1} excitations (Figure 6f,g) are similar to those observed for *p*-methoxyphenol with regard to the Franck–Condon activity and spectral congestion. Figure 6h is the DF spectrum of the 976 cm^{-1} excitation, which is a $15_0^1 1_0^1$ combination band. A significant amount of spectral congestion is also observed to the red of the band origin, which is suggestive of IVR. Shown in Figure 6i is the DF spectrum of the 1302 cm^{-1} ($7a_0^1$) excitation. This spectrum is a bare continuum void of any discrete transitions, indicating dissipative IVR.

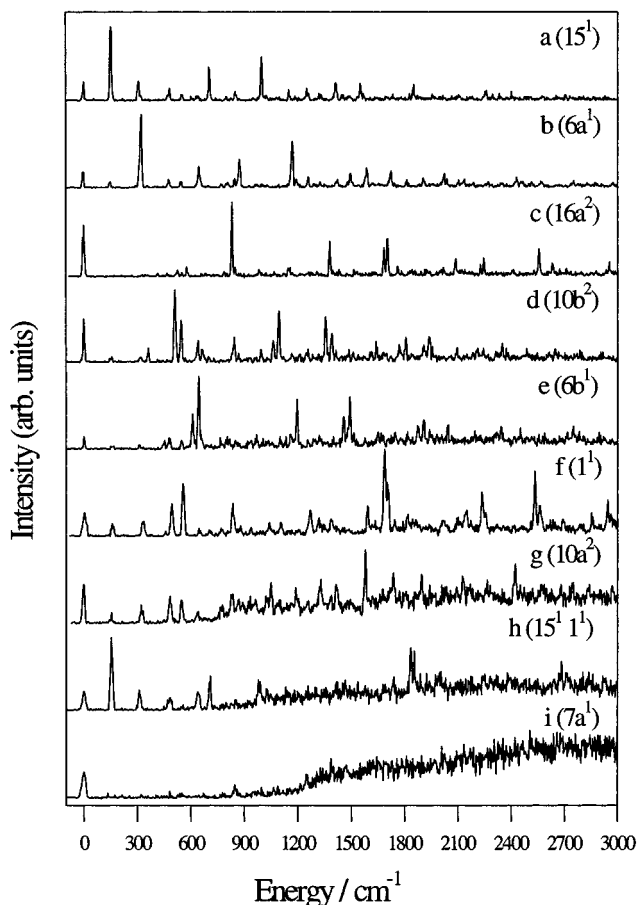


Figure 6. Dispersed fluorescence spectra following excitation of the (a) 163, (b) 326, (c) 359, (d) 527, (e) 575, (f) 828, (g) 851, (h) 976, and (i) 1302 cm^{-1} transitions of *trans-p*-ethoxyphenol. The band-pass of monochromator was 10 cm^{-1} for a–e and 15 cm^{-1} for f–i. For better presentation, the excitation transitions are aligned, and the spectra are plotted on a relative energy scale.

Figure 7 shows the DF spectra of various vibronic excitations of *cis*-ethoxyphenol. Traces a–d of Figure 7 are for the corresponding excitations of its trans counterpart. They were remarkably similar, except that, for the $10b_0^2$ DF spectrum (Figure 7d), the $16b_1^1$ transition at 518 cm^{-1} is missing. The DF spectrum of 1_0^1 (814 cm^{-1}) is presented in Figure 7e. The Franck–Condon activity in the excited mode is slightly different compared to that of its trans counterpart, i.e., the intensity in the resonance transition is significantly higher. Some amount of spectral congestion is also observed, which can be attributed to IVR. The DF spectrum of the 826 cm^{-1} excitation (Figure 7f) shows a striking resemblance to the 829 cm^{-1} excitation of *p*-methoxyphenol, and it can be deduced that these two molecules have a similar mode-mixing pattern in the excited state. The spectrum presented in Figure 7g is the DF spectrum of the $6a_0^1$ and $10b_0^2$ combination band (835 cm^{-1}). Although a reasonable amount of spectral congestion is present, the intensity in the discrete transitions is more than that for its trans counterpart. Figure 7h shows the DF spectrum of the 916 cm^{-1} ($18a_0^1$) excitation, which has very little intensity in the discrete transitions, indicating that IVR is dissipative at this energy.

4. Discussion

From the excitation spectra (Figure 1), it is evident that the Franck–Condon activity progressively changes down the series with the substitution of the phenolic hydrogen in hydroquinone

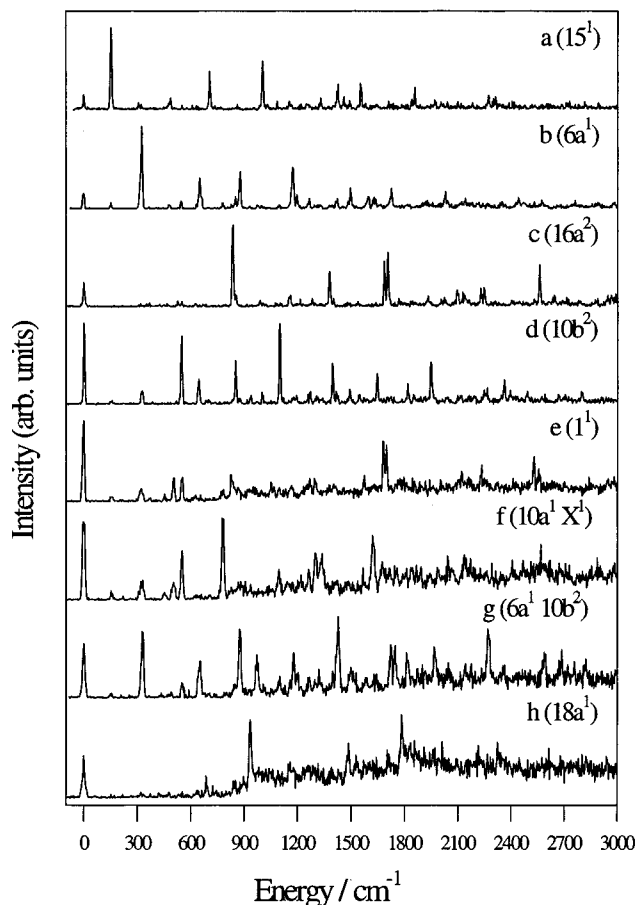


Figure 7. Dispersed fluorescence spectra following excitation of the (a) 149, (b) 316, (c) 340, (d) 519, (e) 814, (f) 826, (g) 835, and (h) 916 cm^{-1} transitions of *cis-p*-ethoxyphenol. The band-pass of monochromator was 10 cm^{-1} for a–e and 15 cm^{-1} for f–h. For better presentation, the excitation transitions are aligned, and the spectra are plotted on a relative energy scale.

with a methyl group in *p*-methoxyphenol and an ethyl group in *p*-ethoxyphenol. In hydroquinone, the entire spectrum consists of transitions involving mainly three totally symmetric modes, viz., 6a, 1, and 7a, and a progression in mode 6a on the band origin and in combination with modes 1 and 7a. In *p*-methoxyphenol and *p*-ethoxyphenol, the number of transitions increases, some of which are $\Delta\nu = 1$ transitions in non-totally symmetric modes, indicating a lowering of the symmetry from C_{2v} to C_s . Also, the Franck–Condon activity in the latter two compounds is mainly concentrated in the $\Delta\nu = 0$ transitions, as is evident from the relatively strong band origins compared to the other transitions. In both of these compounds, there were hardly any discernible transitions beyond 1500 cm^{-1} in the excitation spectra (not shown in the figure). As far as the *cis* and *trans* isomers are concerned, the *trans* isomer was found to be lower in energy in all three compounds. In hydroquinone, it was only marginally lower, i.e., by 32 cm^{-1} , but in *p*-methoxyphenol and *p*-ethoxyphenol the separation between the *cis* and *trans* isomer band origins increased to $\sim 105 \text{ cm}^{-1}$.

A similar trend was also observed in the DF spectra of the three compounds (Figure 2). For instance, the progression in 6a shortened significantly from $\nu'' = 6$ in hydroquinone to $\nu'' = 2$ in *p*-ethoxyphenol. In fact, the Franck–Condon activity in this mode was also found to be quite contrasting in hydroquinone and *p*-methoxyphenol/*p*-ethoxyphenol, as shown in Figure 8. The $\Delta\nu = 0$ transition is the weakest in hydroquinone, indicating a large shift in the 6a potential in the S_1 state. In the

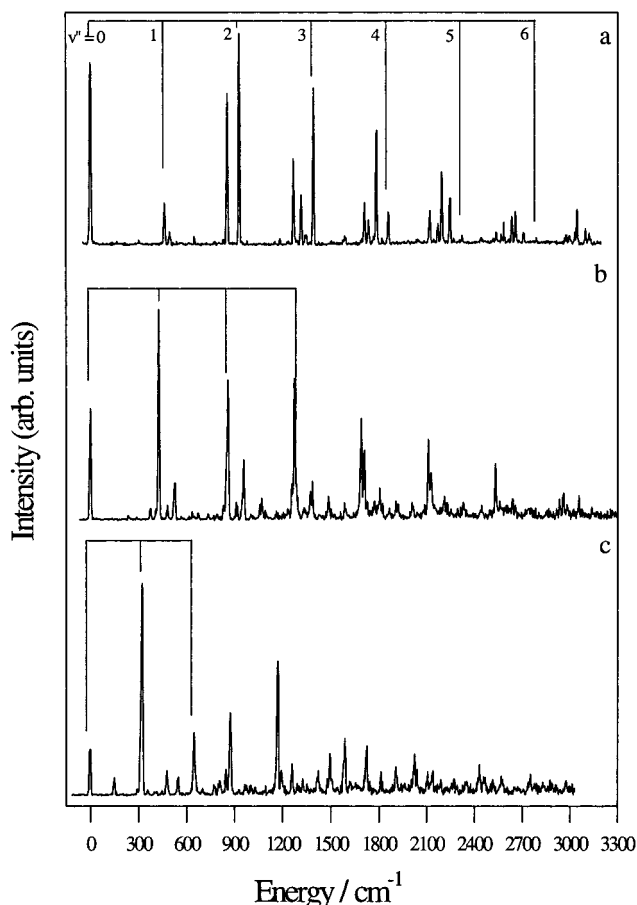


Figure 8. Dispersed fluorescence spectra of the $6a_0^1$ excitation of (a) *trans*-hydroquinone, (b) *trans-p*-methoxyphenol, and (c) *trans-p*-ethoxyphenol. The band-pass of the monochromator was 10 cm^{-1} for all of the spectra. For better presentation, the excitation transitions are aligned, and the spectra are plotted on a relative energy scale.

case of *p*-ethoxyphenol, it was not only the strongest peak, but also acted as the pseudo-origin for the rest of the spectrum, a characteristic of a potential that is very similar in the S_0 and the S_1 states. Because mode 6a samples quinoidal geometry at one of its turning points, the abrupt lowering of the 6a progression in *p*-methoxyphenol can be related to the diminished quinoidal character in its excited state. The DF spectra of the isomers of hydroquinone for various excitations are nearly identical. However, in *p*-methoxyphenol and *p*-ethoxyphenol, the Franck–Condon activity in a few select modes is found to be distinctly different in their respective isomers, *vide supra*. All of the above observations can be summarized as follows. There are no significant differences in the electronic structures of the *cis* and the *trans* isomers of all three compounds. Down the series of molecules, the electronic structure in the S_1 state changes progressively, the largest change being between hydroquinone and methoxyphenol. The most striking difference is in the Franck–Condon activity in the 6a mode, which samples the benzenoidal and the quinoidal structures at its classical turning points. Therefore, it can be inferred that, in hydroquinone, the S_1 state assumes significant quinoidal structure, which diminishes dramatically upon substitution of the phenolic hydrogen. These observations are very similar to those for the case of the *p*-alkoxyaniline series.^{25,28}

Dispersed fluorescence spectra provide useful information about the extent of zero-order mixing, a precursor of IVR, in the excited state. An increased number of transitions or spectral congestion in the fluorescence spectrum indicates that the

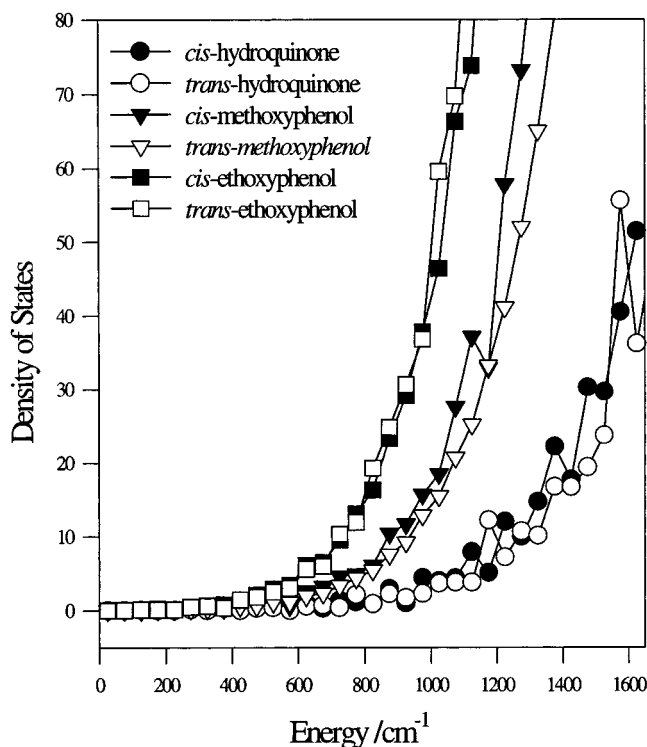


Figure 9. Plot of density of states vs vibrational energy for the trans and cis isomers of hydroquinone, *p*-methoxyphenol, and *p*-ethoxyphenol (see text for details).

initially excited level is coupled to a few of the bath levels, and under appropriate conditions (coherent excitation of the entire envelope), IVR will take place. In an extreme situation where no resonance fluorescence at the excitation wavelength is observed and the fluorescence spectrum is a bare continuum, a large number of zero-order states are mixed with the initially excited level, leading to dissipative IVR.

From the observed spectral characteristics of the dispersed fluorescence spectra, the onset of IVR in the hydroquinone isomers was set around 1650 cm^{-1} (Figure 3). In the case of the *p*-methoxyphenol isomers, it decreases to around 800 cm^{-1} (Figures 4 and 5). In *p*-ethoxyphenol, it does not decrease any further, and qualitatively speaking, even the extent of IVR is not any more than that observed in the case of *p*-methoxyphenol. The IVR process depends on the density of states of the bath levels and the extent of mixing, or the coupling matrix elements. The second factor depends on the electronic structure of the molecule. Another factor that influences IVR under specific experimental conditions is the presence of internal rotors. However, it has been shown that a methyl rotor does not contribute significantly to the process of IVR under supersonic jet-expansion conditions, because of the lack of population in the free rotor levels in the ground state.^{15,17,25}

The densities of states of both of the isomers of hydroquinone, *p*-methoxyphenol, and *p*-ethoxyphenol were calculated using the seven-frequency model³⁸ at 50 cm^{-1} intervals. The vibrational frequencies used for this purpose were calculated with Gaussian 94³⁹ using 6-31G* basis set at the RCIS level and were scaled by a factor of 0.9. Figure 9 shows a plot of the total state density vs energy in the S_1 state. The densities of states for both of the isomers of all three molecules are nearly equal at all energies. The density of states for hydroquinone at around 1650 cm^{-1} is a factor of 10 greater than that at 800 cm^{-1} in the case of *p*-methoxyphenol. Further, the density of states in the case of *p*-ethoxyphenol at 800 cm^{-1} is about two

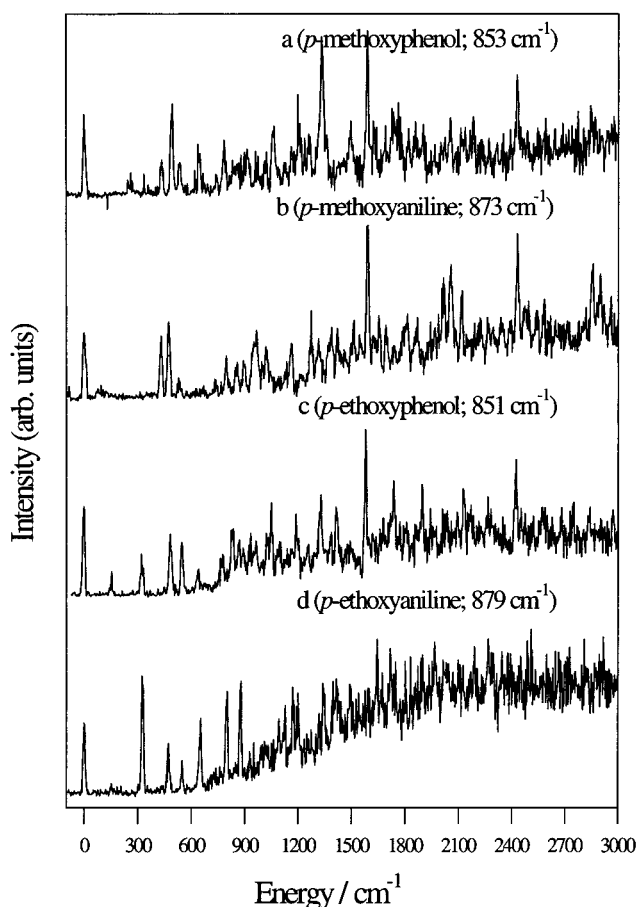


Figure 10. Dispersed fluorescence spectra of vibronic excitations at $\sim 850\text{ cm}^{-1}$ of (a) *trans-p*-methoxyphenol, (b) *p*-methoxyaniline, (c) *trans-p*-ethoxyphenol, and (d) *p*-ethoxyaniline. The band-pass of the monochromator was 15 cm^{-1} for all of the spectra. For better presentation, the excitation transitions are aligned, and the spectra are plotted on a relative energy scale.

times greater that of *p*-methoxyphenol at same energy. If the Fermi golden rule is invoked, it can be inferred that coupling between the excited mode and bath modes in *p*-methoxyphenol is significantly greater compared to that in hydroquinone, but only marginally greater than that in *p*-ethoxyphenol. The increase in the vibronic coupling for *p*-methoxyphenol and *p*-ethoxyphenol is attributed to the substantial reduction in the quinoidal character in their S_1 states. Given the fact that the $-\text{OH}$ fragment in hydroquinone does not have many low-frequency modes, the exact role of quinoidal character in arresting IVR must be understood properly. We reported earlier²⁵ a comparative study of IVR behavior in molecules with similar densities of states but varying quinoidal character, viz., *p*-aminophenol and *p*-aminobenzonitrile. The findings were that, for the latter compound, the IVR onset was observed at around 800 cm^{-1} compared to that at 1150 cm^{-1} for *p*-aminophenol, which has a greater amount of quinoidal character. This observation, along with that in the present series, strongly suggests that vibronic coupling not only to the substituent modes alone, but also to the low-frequency ring modes, becomes arrested because of the presence of quinoidal character. If this trend were to continue further, then, in *p*-ethoxyphenol, coupled with its greater density of states, one would expect that the onset of IVR will be further lowered. However, the onset of IVR in the case of *p*-ethoxyphenol does not decrease further, i.e., it is around the same energy at which the onset was found for *p*-methoxyphenol.

Earlier, we reported IVR in the *p*-alkoxyaniline series.²⁹ The onset of IVR in the first member, *p*-aminophenol was around 1130 cm⁻¹, and even up to 1600 cm⁻¹, it was found to be restrictive in nature. It lowered to ~800 cm⁻¹ in *p*-methoxyaniline, which was noncommensurate with the density of states. The onset further lowered for *p*-ethoxyaniline, as expected on the basis of increased state density. In the present context, the onset of IVR in the case of hydroquinone was at significantly higher energy than that in *p*-aminophenol. This suggests that the S₁ state of hydroquinone must be more quinoidal than *p*-aminophenol even though the progression in mode 6a is comparable in both cases. Because the length of a progression depends only on the shift in the potentials of the S₁ and S₀ states, it can be deduced that, for hydroquinone, the S₀ state itself has greater quinoidal character than that in *p*-aminophenol. Figure 10 shows a comparison of the DF spectra of the vibronic excitations around 850 cm⁻¹ for *p*-methoxy- and *p*-ethoxyphenols and anilines. Figure 10a is the DF spectrum of the 854 cm⁻¹ excitation of *trans-p*-methoxyphenol, and 10b is the corresponding spectrum of *p*-methoxyaniline. It can be seen that the number of discrete transitions and the ratio of the discrete transitions to the continuum are greater in the case of *p*-methoxyphenol than in *p*-methoxyaniline. A similar situation holds for the ethoxy derivatives (Figure 10c,d). Moreover, it can also be seen that the amount of spectral congestion in *p*-methoxyaniline is comparable to that in *p*-ethoxyphenol. Although the trend is similar in both series, the extent of IVR in *p*-alkoxyphenols is less than that in *p*-alkoxyanilines. The DF spectrum for the 852 cm⁻¹ excitation of *p*-ethoxyaniline can be classified as dissipative, whereas that of *p*-ethoxyphenol falls under the restrictive category. This difference could be attributed to the presence of the phenolic group in the para position in the case of *p*-alkoxyphenols. Although IVR behavior in the present series shows a trend similar to that in the aniline series for the first two members, the IVR in the ethoxy analogue is quite different. The similarity in the extent of IVR and its onset in *p*-methoxyphenol and *p*-ethoxyphenol is not clearly understood. The IVR investigations of the higher members of the *p*-alkoxyphenol series must be carried out to understand this behavior.

5. Conclusions

Table 4 gives the vibronic assignments in the S₁ and the S₀ states for both of the isomers of all three molecules. The spectroscopy of the respective isomers is very similar, barring a few vibrational modes. The electronic structure in the excited state progressively changes from hydroquinone to *p*-ethoxyphenol. The IVR onset in hydroquinone was observed at 1650 cm⁻¹, and it decreased significantly to around 800 cm⁻¹ in the case of *p*-methoxyphenol. In *p*-ethoxyphenol, it did not decrease any further. Isomer dependence of IVR was not observed. The spectroscopy and the IVR trend in this series are quite parallel to those in the case of *p*-alkoxyanilines; however, the extent of IVR in the present series is lesser than that in the latter. This was attributed to the presence of the phenolic OH group in the para position.

Acknowledgment. The authors are grateful to Prof. S. V. K. Kumar and Dr. Nandini Bhattacharya for the loan of the monochromator.

References and Notes

- (1) Brown, S. S.; Metz, R. B.; Berghout, H. C.; Crim, F. F. *J. Chem. Phys.* **1996**, *105*, 6293.
- (2) Metz, R. B.; Thoemke, J. D.; Pfeiffer, J. M.; Crim, F. F. *J. Chem. Phys.* **1993**, *99*, 1744.
- (3) Sinha, A.; Thoemke, J. D.; Crim, F. F. *J. Chem. Phys.* **1992**, *96*, 372.
- (4) Simpson, W. R.; Girard, B.; Zare, R. N. *J. Chem. Phys.* **1991**, *95*, 8647.
- (5) Bar, I.; Cohen, Y.; David, D.; Rosenwaks, S.; Valentini, J. *J. Chem. Phys.* **1990**, *93*, 2146.
- (6) Hopkins, J. B.; Powers, D. E.; Smalley, R. E. *J. Chem. Phys.* **1980**, *72*, 5039.
- (7) Hopkins, J. B.; Powers, D. E.; Mukamel, S.; Smalley, R. E. *J. Chem. Phys.* **1980**, *72*, 5049.
- (8) Hopkins, J. B.; Powers, D. E.; Smalley, R. E. *J. Chem. Phys.* **1980**, *73*, 683.
- (9) Powers, D. E.; Hopkins, J. B.; Smalley, R. E. *J. Chem. Phys.* **1980**, *72*, 5721.
- (10) Hopkins, J. B.; Powers, D. E.; Smalley, R. E. *J. Chem. Phys.* **1981**, *74*, 6986.
- (11) Powers, D. E.; Hopkins, J. B.; Smalley, R. E. *J. Chem. Phys.* **1981**, *74*, 5971.
- (12) Ebata, T.; Ito, M. *J. Phys. Chem.* **1992**, *96*, 3224.
- (13) Gruner D.; Brumer, P. *J. Chem. Phys.* **1991**, *94*, 2848; **1991**, *94*, 2862.
- (14) Coveleskie, R. A.; Dolson, D. A.; Parmenter, C. S. *J. Phys. Chem.* **1985**, *89*, 654; **1985**, *89*, 655.
- (15) Baskin, J.; Rose, T. S.; Zewail, A. H. *J. Chem. Phys.* **1989**, *88*, 1458.
- (16) Zhang, X.; Smith, J. M.; Knee, J. L. *J. Chem. Phys.* **1994**, *100*, 2429.
- (17) Parmenter, C. S.; Stone, B. M. *J. Chem. Phys.* **1986**, *84*, 4710.
- (18) Hickman, C. G.; Gascooke, J. R.; Lawrance, W. D. *J. Chem. Phys.* **1996**, *104*, 4887.
- (19) Yu, H.; Joslin, E.; Crystall, B.; Smith, T.; Sinclair, W.; Philips, D. *J. Phys. Chem.* **1993**, *97*, 8146.
- (20) Takayanagi, M.; Hanazaki, I. *Laser Chem.* **1993**, *14*, 103.
- (21) Gibson, E. M.; Jones, A. C.; Taylor, A. G.; Bouwman, W. G.; Philips, D.; Sandell, J. *J. Phys. Chem.* **1988**, *92*, 5449.
- (22) Yu, H.; Joslin, E.; Philips, D. *J. Chem. Soc., Faraday Trans.* **1993**, *89*, 2345.
- (23) Song, X.; Wilkerson, C. W., Jr.; Lucia, J.; Pauls, S.; Reilly, J. P. *Chem. Phys. Lett.* **1990**, *174*, 377.
- (24) Weersink, R. A.; Wallace, S. C. *J. Chem. Phys.* **1993**, *97*, 6127.
- (25) Wategaonkar, S.; Doraiswamy, S. *J. Chem. Phys.* **1996**, *105*, 1786.
- (26) Patwari, G. N.; Doraiswamy, S.; Wategaonkar, S. *Chem. Phys. Lett.* **2000**, *316*, 433.
- (27) Yan, S.; Spangler, L. H. *J. Chem. Phys.* **1992**, *96*, 4106.
- (28) Wategaonkar, S.; Doraiswamy, S. *J. Chem. Phys.* **1997**, *106*, 4894.
- (29) Patwari, G. N.; Doraiswamy, S.; Wategaonkar, S. *Phys. Chem. Chem. Phys.* **1999**, *1*, 2789.
- (30) Dunn, T. M.; Tumbrell, R.; Lubman, D. M. *Chem. Phys. Lett.* **1985**, *121*, 453.
- (31) Tumbrell, R.; Dunn, T. M.; Lubman, D. M. *Spectrochim. Acta* **1986**, *42A*, 899.
- (32) Oikawa, A.; Abe, H.; Mikami, N.; Ito, M. *Chem. Phys. Lett.* **1985**, *116*, 50.
- (33) Humphrey, S. J.; Pratt, D. W. *J. Chem. Phys.* **1986**, *99*, 5078.
- (34) Baskin, J. E.; Dantus, M.; Zewail, A. H. *Chem. Phys. Lett.* **1986**, *130*, 473.
- (35) Patwari, G. N.; Doraiswamy, S.; Wategaonkar, S. *Chem. Phys. Lett.* **1998**, *289*, 8.
- (36) Tzeng, W. B.; Narayanan, K.; Hsieh, C. Y.; Tung, C. C. *J. Mol. Struct.* **1998**, *448*, 91.
- (37) Varsanyi, G. *Assignments of Vibrational Spectra of Seven Hundred Benzene Derivatives*; Wiley: New York, 1974; Vol. 1.
- (38) Robinson P. J.; Holbrook, K. A. *Unimolecular Reactions*; Wiley: New York, 1972.
- (39) Frisch, M. J.; Trucks, G. W.; Schlegel, H. B.; Gill, P. M. W.; Johnson, B. G.; Robb, M. A.; Cheeseman, J. R.; Keith, T.; Petersson, G. A.; Montgomery, J. A.; Raghavachari, K.; Al-Laham, M. A.; Zakrzewski, V. G.; Ortiz, J. V.; Foresman, J. B.; Cioslowski, J.; Stefanov, B. B.; Nanayakkara, A.; Challacombe, M.; Peng, C. Y.; Ayala, P. Y.; Chen, W.; Wong, M. W.; Andres, J. L.; Replogle, E. S.; Gomperts, R.; Martin, R. L.; Fox, D. J.; Binkley, J. S.; Defrees, D. J.; Baker, J.; Stewart, J. P.; Head-Gordon, M.; Gonzalez, C.; Pople, J. A. *Gaussian 94*, revision C.2; Gaussian, Inc.: Pittsburgh, PA, 1995.